Journal of Materials Science and Chemical Engineering, 2023, 11, 61-85
https://www.scirp.org/journal/msce
ISSN Online: 2327-6053
ISSN Print: 2327-6045

Localized Theoretical Analysis of Thermal Performance of Individually Finned Heat Pipe Heat Exchanger for Air Conditioning with Freon R404A as Working Fluid

Élcio Nogueira

Department of Mechanic and Energy, State University of Rio de Janeiro, Rio de Janeiro, Brazil
Email: elcionogueira@hotmail.com

How to cite this paper: Nogueira, É. (2023) Localized Theoretical Analysis of Thermal Performance of Individually Finned Heat Pipe Heat Exchanger for Air Conditioning with Freon R404A as Working Fluid. *Journal of Materials Science and Chemical Engineering*, **11**, 61-85.
https://doi.org/10.4236/msce.2023.118005

Received: June 24, 2023
Accepted: August 28, 2023
Published: August 31, 2023

Abstract

This work contributes to the improvement of energy-saving in air conditioning systems. The objective is to apply the thermal efficiency of heat exchangers for localized determination of the thermal performance of heat exchangers with individually finned heat pipes. The fundamental parameters used for performance analysis were the number of fins per heat pipe, the number of heat pipes, the inlet temperatures, and the flow rates of hot and cold fluids. The heat exchanger under analysis uses Freon 404A as a working fluid in an air conditioning system for cooling in the Evaporator and energy recovery in the Condenser. The theoretical model is localized and applied individually to the Evaporator, Condenser, and heat exchanger regions. The results obtained through the simulation are compared with experimental results that use a global approach for the heat exchanger. The thermal quantities obtained through the theoretical model in the mentioned regions are air velocity, Nusselt number, thermal effectiveness, heat transfer rate, and outlet temperature. The comparisons made with global experimental results are in excellent agreement, demonstrating that the localized theoretical approach developed is consistent and can be used as a comprehensive analysis tool for heat exchangers using heat pipes.

Keywords

Individually Finned Heat Pipe, Heat Exchanger, Thermal Efficiency, Thermal Effectiveness, Air Conditioning, Freon R404A

1. Introduction

Grzegorz Górecki *et al.* [1] present a global theoretical-experimental study of a

heat pipe heat exchanger used for energy recovery in air conditioning systems. The heat pipe set is individually finned. They use R404A refrigerant with a filling rate equal to 20%. The computational analysis, using parametric calculations, made it possible to conclude that 20 lines of heat pipes allow an efficiency equal to 60%. Furthermore, the heat exchanger designed and tested experimentally showed a reasonable level, with a maximum absolute relative error of 10%.

Nandy Putra *et al.* [2] performed an experimental study on Heating, Ventilation, and Air Conditioning (HVAC) systems for hospitals to ensure the air quality in terms of temperature and humidity and are free from toxic waste. The study aimed to investigate the performance of heat pipes in recovering energy through exhaust air from an operating room, where a heat pipe heat exchanger (PHE) is highly recommended. Therefore, experiments were performed to evaluate the effect of evaporator inlet temperature, the number of heat pipelines, and air velocity on energy conservation. As a result, it was observed that there is better performance of HPHE for higher air inlet temperatures and that energy consumption decreases from 0.6 to 4.1 GJ/Year.

Hussam Jouhara *et al.* [3] evaluate heat exchanger performance in multi-pass heat pipes in a staggered configuration. The theoretical-experimental procedure transfers energy from hot air traveling through the evaporator section to water, which cools the condenser section. To analyze the overall performance of the heat exchanger, the authors change the number of passes for the evaporator section by including baffles and the water flow rate. With an increase in the number of passes from 1 to 5, the effectiveness increased by 25%. The global theoretical model showed deviations between 15.5% (LMTD) and 19.0% (ε-NTU) concerning the experimental results, predicting values for water output in the Condenser with an accuracy of 0.7%. They emphasize the importance of research on waste heat recovery through heat pipe heat exchangers.

Imansyah Ibnu Hakim *et al.* [4] investigated using a U-shaped finned heat exchanger as pre-cooling to reduce cooling energy and recover residual energy in heating air from the operating room in an air conditioning system. The experimental tests of the system under analysis were carried out in one- and two-row heat pipe configurations, with eight heat pipes per row. They conclude that the U-shaped HPHE increases performance by equal to 39.9% compared to the HVAC without heat pipes and that it becomes a viable solution for fresh air pre-cooling and energy recovery.

Ragil Sukarno *et al.* [5] air quality is a crucial factor in hospital operating rooms, where thermal comfort is one of the relevant aspects. In this sense, the development of heating, ventilation, and air conditioning (HVAC) systems for operating rooms requires efficiency and reliability regarding the temperature in the room, which must remain within a restricted temperature range. The authors present experimental results of an air conditioning system that uses finned heat pipes, with four heat pipes per row, arranged in a staggered configuration. The theoretical validation of the experiment is carried out through a global model using the concept of thermal effectiveness and the number of thermal

units (ε-NTU), which makes it possible to predict, in addition to thermal efficiency, the outlet temperatures in the Condenser. Experimentally, they found that energy recovery increases with the number of rows of heat pipes, increasing temperature and speed at the evaporator inlet.

H. Jouhara *et al.* [6] present a comprehensive review of applications associated with heat pipes, including discussions of the materials in which they are made and their respective performances. First, the study addresses heat pipes used at low and high temperatures, working fluids and their respective operating temperatures, coating materials, and thermal modeling. Next, they focus on solar applications, nuclear engineering, thermal and ceramic modules, nanoparticles, and heat pipe modeling. The last aspect covers technical aspects, and internal and external thermal modeling methodologies, for Newtonian, non-Newtonian, and nanofluids. In addition, they discuss the limitations of heat pipes, such as operational limitations and lack of empirical information that can help in the modeling process.

Ayad S. Abedalh *et al.* [7] present experimental work to test heat pipe heat exchanger HPHE composed of 40 heat pipes arranged in four lines, with internal and external diameters equal to 1 cm and 1.23 cm, and with distilled water as the working fluid. The Evaporator is filled with 50% of the volume. The HPHE is air conditioning tested. The air speeds and temperature at the inlet of the Evaporator and Condenser are the parameters used to evaluate the outlet temperatures. Additional data obtained through the experiment were the effectiveness of the heat exchanger and the energy recovery rate. The highest value reached for effectiveness was 64.6%, with an inlet velocity equal to 1.0 m/s, and the highest value of energy recovered, equal to 923.4 W, corresponds to the inlet temperature of the Evaporator equal to 33.6˚C.

Mostafa A. Abd El-Baky and Mousa M. Mohamed [8] evaluated an experimental configuration of a heat pipe heat exchanger—HPHE. The fresh air temperature at the evaporator inlet ranged from 32˚C to 40˚C. They observed that heat transfer efficiency in the evaporator and condenser sections increased by 48% for an inlet temperature equal to 40˚C compared to an inlet temperature equal to 30˚C. They also observed that the energy recovery is about 85% with the fresh air inlet temperature increase and that the efficiency is close to the maximum possible.

Anwar Barrak [9] related that with the increase in energy demand, many researchers have focused on recovering wasted heat and devices capable of performing the task efficiently. The results obtained in recent years have shown that heat pipe heat exchangers—HPHE are suitable devices for energy recovery. In this sense, the authors experimentally investigate each type of heat pipe, *i.e.*, conventional heat pipe, thermosyphon pipe, and oscillating heat pipe. They contain three sections: the Evaporator, the adiabatic, and the Condenser. Anwar Barrak concluded that the heat pipe heat exchanger as a heat recovery device had been successfully applied in the HVAC system to increase energy saving, cooling

coil capacity, and dehumidification capacity. However, despite the achievements obtained with theoretical studies, the mass and heat transfer mechanism in the operation of the OHP have not yet been fully understood. Moreover, some issues still need further investigation, like the chaotic behavior in the heat pipe, the hydrodynamic and thermodynamic effects on thermal performance, and the mechanism of heat and mass formation and transfer between liquid plugs and steam slugs. Finally, the design techniques for heat pipe heat exchange currently do not have a reliable method.

T. Höhne [10] states that heat pipes improve the thermal performance of heat exchangers and enable energy savings. It uses computational fluid dynamics (CFD) to simulate the two-phase phase in the heat transfer process in heat pipes, using a homogeneous multiphase model and visual aids in three dimensions (3D). Comparisons of the implemented model with experimental results showed reasonable agreement, provided that the heating power does not exceed 1000 W for the type of copper heat pipe analyzed. He mentions that future numerical models will be applied more frequently in his conclusions.

2. Methodology

The system under analysis consists of a heat exchanger with individually finned heat pipes. The evaporator region is used for air cooling and the condenser region as energy recovery. The configuration under analysis was taken from theoretical-experimental work presented through reference [1]. The experiment was designed so that the configuration of the heat pipes is in a staggered formation. Therefore, the number of heat pipes varies depending on the number of rows being analyzed, and they are multiples of 7 pipes. The number of fins per heat pipe used in the experiment was not made explicit.

Figure 1(a) presents the geometry of the Individually Finned Heat Tube—IFHPHE, and **Figure 1(b)** presents the basic configuration of the heat exchanger, with a row of four heat pipes and a row of three heat pipes. The number of heat pipes ranges from 7 to 49, and the number of rows from 3 to 21. The number of fins per heat pipe ranges from 0 to 70 in the theoretical model. The experimental work used as a reference [1] does not specify the number of fins per heat pipe.

$$T_{sat} = 17.0^{\circ}\text{C fixed by definition} \tag{1}$$

Equation (1) represents the saturation temperature of the working fluid (R404A) in the heat pipe.

The saturation pressure of the working fluid (R404A) can be obtained through Equation (2):

$$P_{sat} = 614.1316315 + 17.18802462T_{sat} + 0.3276728108T_{sat}^2 \tag{2}$$

The properties of the working fluid (R404A) can be obtained by Equations (3)-(21):

$$\rho_l = 1148.516119 - 2.934024895T_{sat} - 0.0425519003T_{sat}^2 \tag{3}$$

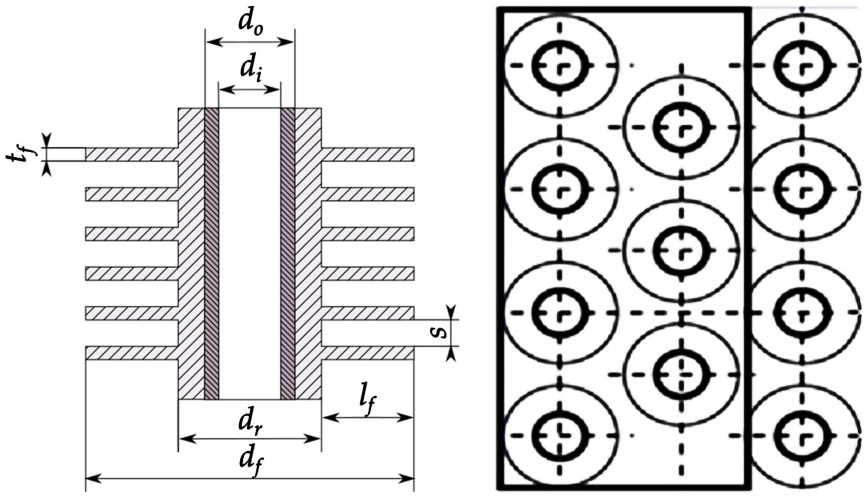

(a) (b)

Figure 1. (a) Geometric parameters of Individually Finned Heat Tube-IFHPHE [1]; (b) Basic configuration: 7 heat pipes (4 + 3) [1].

$$\rho_v = 29.62609253 + 1.088373933T_{sat} + 0.002241182059T_{sat}^2 + 0.0003618637607T_{sat}^3 \quad (4)$$

$$h_l = 200.2774524 + 1.356658428T_{sat} + 0.00586628846T_{sat}^2 \quad (5)$$

$$h_v = 368.3562439 + 0.5331782112T_{sat} - 0.0005307756065T_{sat}^2 - 6.0092036610^{-5}T_{sat}^3 \quad (6)$$

$$h_{lv} = h_v - h_l \quad (7)$$

$$k_{R404l} = 0.0863\frac{\mathrm{W}}{\mathrm{m}\cdot\mathrm{K}} \quad (8)$$

$$k_{R404v} = 0.01346 \quad (9)$$

$$Cp_{R404l} = 1530 \quad (10)$$

$$Cp_{R404v} = 870 \quad (11)$$

$$\mu_{R404l} = 1.28\times10^{-4} \quad (12)$$

$$\mu_{R404v} = 1.22\times10^{-5} \quad (13)$$

$$\nu_{R404l} = \frac{\mu_{R404l}}{\rho_{R404l}} \quad (14)$$

$$\nu_{R404v} = \frac{\mu_{R404v}}{\rho_{R404v}} \quad (15)$$

$$\alpha_{R404l} = \frac{k_{R404l}}{\rho_{404l}Cp_{404l}} \quad (16)$$

$$\alpha_{R404v} = \frac{k_{R404v}}{\rho_{404v}Cp_{404v}} \quad (17)$$

$$Pr_{R404l} = \frac{\nu_{R404l}}{\alpha_{R404l}} \quad (18)$$

$$Pr_{R404v} = \frac{\nu_{R404v}}{\alpha_{R404v}} \tag{19}$$

The number of rows of HP is defined by Equation (22).

$$N_{rows} = 3 \text{ default } [1]; \quad 3 \le N_{rows} \le 21 \tag{20}$$

$$NHP = \frac{N_{rows}}{3}(3+4); 7 \le NHP \le 49 \tag{21}$$

$$N_{Fin} = 30 \text{ default}; 0 \le N_{Fin} \le 70 \tag{22}$$

$$\dot{V}_{air} = \frac{370.0}{3600}\frac{\text{m}^3}{\text{s}} \text{ default}; \frac{370.0}{3600} \le \dot{V}_{air} \le \frac{550.0}{3600} \tag{23}$$

Equation (23) represents the total number of heat pipes in the heat exchanger. The number of fins considered in the Evaporator or condenser is defined by Equation (24). The volume flow rate of the air is represented by Equation (25).

The properties of the air, dependent on the inlet temperature, can be obtained by the following Equations (26)-(29):

$$k_{air} = 6.91744186 \times 10^{-5} Tair_{in} + 0.02462173663 \tag{24}$$

$$\begin{aligned} \mu_{air} = {} & 1.95483621 \times 10^{-5} + 2.735058039 \times 10^{-9} Tair_{in} \\ & + 2.309587479 \times 10^{-10} Tair_{in}^2 - 4.505882353 \times 10^{-13} Tair_{in}^3 \end{aligned} \tag{25}$$

$$\begin{aligned} Cp_{air} = {} & 1003.728948 + 0.06727399886 * Tair_{in} + 3.565918367 \times 10^{-6} Tair_{in}^2 \\ & + 8.222222222 \times 10^{-7} Tair_{in}^3 \end{aligned} \tag{26}$$

$$\begin{aligned} \rho_{air} = {} & 1.219135515 - 0.002152770329 Tair_{in} - 3.64047479 \times 10^{-7} Tair_{in}^2 \\ & + 1.705882353 \times 10^{-9} Tair_{in}^3 \end{aligned} \tag{27}$$

Equation (26) is represented by thermal conductivity. Equation (27) is characterized by the dynamic, absolute viscosity of air. Equation (28) is represented by the specific heat of air. Equation (29) is represented by the density of the air.

$$\nu_{air} = \frac{\mu_{air}}{\rho_{air}} \tag{28}$$

$$\alpha_{air} = \frac{k_{air}}{\rho_{air} Cp_{air}} \tag{29}$$

$$Pr_{air} = \frac{\nu_{air}}{\alpha_{air}} \tag{30}$$

Equation (32) is represented by the Prandtl number associated with the air.

Equation (33) is the surface tension for water:

$$\sigma_{Water} = 0.07275d0\left(1 - 0.002d0\left(K - 291\right)\right) \tag{31}$$

where K is the saturation temperature in Kelvin.

$$C_{sf} = 0.006 \tag{32}$$

Equation (34) is represented by the assumed constant for the surface-fluid combination.

$$\dot{m}_{air} = \rho_{air} \dot{V}_{air} \tag{33}$$

The mass flow rate of air at the inlet of the heat exchanger is defined by Equation (35).

The localized analytical approach is subdivided into the evaporator, the condenser, and the global IFHPHE.

2.1. Evaporator Section of the Heat Exchanger

In the evaporator region, the cooling of the heated fresh air, the inlet temperature of heated fresh air varies between 20˚C and 50˚C. The inlet volume flow rate of fresh heated air in the evaporator region varies between 0.1078 m^3/s and 0.1528 m^3/s.

The formulation to simulate the heat exchange process in the evaporator is established through Equations (36)-(74).

$$TEv_{in} = 30.0^{\circ}\text{C default};\ 20.0^{\circ}\text{C} \le TE_{in} \le 50.0^{\circ}\text{C} \tag{34}$$

The fresh air inlet temperature in the evaporator region, defined by Equation (36), is represented by TEv_{in}.

$$h_{boil} = \mu_l h_{lv} \left(\frac{g(\rho_l - \rho_v)}{\sigma_{water}} \right)^{1/2} \left(\frac{Cp_l}{C_{sf} h_{lv} Pr_l} \right)^3 \Delta T_{sat}^2 \tag{35}$$

The estimated heat transfer coefficient for the boiling process, initially presented by Rohsenow [11] and related by Hussam Jouhara [5], is given by Equation (37) h_{boil}.

$$\Delta T_{Evsat} = TEv_{in} - T_{sat} \tag{36}$$

$$D_{ext} = 22.0 \times 10^{-3}\ \text{m} \tag{37}$$

$$D_{int} = 20.0 \times 10^{-3}\ \text{m} \tag{38}$$

The outside and inside diameters of the heat pipe are represented by D_{ext} and D_{int} given by Equations (39) and (40).

$$k_W = 235.0 \tag{39}$$

The thermal conductivity of the heat pipe material (Copper), represented by Equation (41), is given by k_W.

$$LEv = 250.0 \times 10^{-3} \tag{40}$$

$$WHE = 200.0 \times 10^{-3} \tag{41}$$

LEv, illustrated by Equation (39), is the length of the heat pipe evaporation section and *WHE*, represented by Equation (40), is the shell's width.

$$t_{Fin} = 0.8 \times 10^{-3} \tag{42}$$

$$k_{Fin} = 401.0 \tag{43}$$

The thermal conductivity of the fin material (Aluminum), represented by Equation (42), is given by k_{Fin}.

$$Sp_{Fin} = 2.5 \times 10^{-3}\ \text{ by definition} \tag{44}$$

$$LEv_{effec} = LEv - NFin\left(t_{Fin} + Sp_{Fin}\right) \tag{45}$$

The effective heat exchange length associated with the heat pipes in the evaporator, represented by Equation (44), is obtained LEv_{effec}. The thickness of a fin, represented by Equation (41), is given by t_{Fin}. The space between fins, defined through Equation (43), is provided by Sp_{Fin}.

$$Dh_{EV} = \frac{4WHE \times LEv_{effec}}{2\left(WHE + LEv_{effec}\right)} \tag{46}$$

$$Re_{air} = \frac{4\dot{m}_{air}}{\pi Dh_{Ev}\mu_{air}} \tag{47}$$

The hydraulic diameter of the heat exchanger in the evaporator region is given by Dh_{EV} Equation (45). The Reynolds number associated with air, represented by Equation (46), is provided by Re_{air}.

$$Asec_{air} = \frac{\dot{m}_{air} Dh_{Ev}}{Re_{air}\mu_{air}} \tag{48}$$

Equation (47), represented by $Asec_{air}$, is the effective area occupied by the air in the evaporator.

$$V_{air} = \frac{\dot{m}_{air}}{Asec_{air}\rho_{air}} \tag{49}$$

The air velocity in the evaporator, V_{air}, is represented by Equation (48).

$$Dext_{Fin} = 50.0 \times 10^{-3} \tag{50}$$

$$Dint_{Fin} = D_{ext} \tag{51}$$

$$Atr_{Fin} = NFin \times NHP \frac{\pi}{4}\left(Dext_{Fin}^2 - Dint_{Fin}^2\right) \tag{52}$$

$$Atr_{HP} = NHP\,\pi D_{ext}\left(LEv - NFin \times Sp_{Fin}\right) \tag{53}$$

$$A_{Total} = Atr_{Fin} + Atr_{HP} \tag{54}$$

The effective heat transfer area in the evaporator Atr_{HP}, associated with heat pipes, is established by Equation (52). The effective heat transfer area associated with the fin system, Atr_{Fin}, and the total heat transfer area, A_{Total}, are represented by Equations (51) and (53).

$$Vair_{\max} = \frac{\dot{V}_{air}}{Asec_{air}} \tag{55}$$

$$dr = 24.0 \times 10^{-3} \text{ assumed [1]} \tag{56}$$

$$Re_{dr} = \frac{Vair_{\max} dr}{\nu_{air}} \tag{57}$$

$$Nu_{air} = 0.1387 Re_{dr}^{0.718} Pr_{air}^{1/3}\left(\frac{Sp_{Fin}}{Dext_{Fin} - Dint_{Fin}}\right)^{0.296} \tag{58}$$

$$h_{air} = \frac{Nu_{air} k_{air}}{dr} \tag{59}$$

The Nusselt number for the air, as reported in [1] Nu_{air}, is represented by Equation (57). The convection heat transfer coefficient associated with air in the

evaporator, Equation (58), is given by h_{air}.

$$mL_{Fin} = \sqrt{\frac{2h_{sair}}{k_{Fin}t_{Fin}}}t_{Fin} \tag{60}$$

$$\eta_{Fin} = \frac{\mathrm{Tanh}\left(mL_{Fin}\right)}{mL_{Fin}} \tag{61}$$

The fin efficiency for the evaporator section is defined through Equation (60) by η_{Fin} [12].

$$\beta = \frac{Atr_{Fin}}{A_{Total}} \tag{62}$$

$$\eta'_{Fin} = \beta\eta_{Fin} + \left(1-\beta\right) \tag{63}$$

The efficiency associated with the set of fins in the evaporator, weighted by the area of heat exchange of the fins η'_{Fin}, is represented through Equation (62).

$$Uo_{Ev} = \frac{1}{\frac{1}{h_{boil}} + \frac{D_{ext}-D_{int}}{kW} + \frac{1}{\eta'_{Fin}h_{air}}} \tag{64}$$

The global heat transfer coefficient associated with air in the Evaporator, Uo_{Ev}, is given by Equation (64).

$$C_{Air} = \dot{m}_{air}Cp_{air} \tag{65}$$

The heat capacity of the air in the evaporator, C_{Air}, is given by Equation (65).

$$C_{Ev} = C_{air} \tag{66}$$

$$NTU_{Ev} = \frac{Uo_{Ev}A_{Total}}{CEv} \tag{67}$$

The number of thermal units associated with air in the evaporator, NTU_{Ev}, is given by Equation (67).

$$Fa = \frac{NTU\sqrt{1+C^{*2}}}{2} \quad \text{for cross-flow} \tag{68}$$

The dimensionless number, called "fin analogy", *Fa* is represented by Equation (68) as defined by Ahamad Fakheri [12] and reported by Nogueira, É. [13] [14].

$$\eta_T = \frac{\tanh\left(Fa\right)}{Fa} \tag{69}$$

The thermal efficiency associated with the heat exchanger is η_T [11].

$$\varepsilon_T = \frac{1}{\frac{1}{\eta NTU} + \frac{1+C^*}{2}} \tag{70}$$

The thermal effectiveness related to the heat exchanger is ε_T [11].

The heat exchanger's thermal efficiency depends on two fundamental parameters: NTU e C^*. For the physical conditions under analysis $C^* = 0.0$. Then,

$$Fa_{Ev} = \frac{NTU_{Ev}}{2} \tag{71}$$

$$\eta_{TEv} = \frac{\tanh\left(Fa_{Ev}\right)}{Fa_{Ev}} \tag{72}$$

$$\varepsilon_{TEv} = \frac{1}{\frac{1}{\eta_{TEv} NTU_{Ev}} + \frac{1}{2}} \tag{73}$$

$$\dot{Q}_{Ev} = \frac{C_{Ev} \Delta T_{Evsat}}{\frac{1}{\eta_{TEv} NTU_{Ev}} + \frac{1}{2}} \tag{74}$$

The heat transfer rate between the air and the heat pipe in the evaporating region $\dot{Q}_{Ev}$ is given by Equation (74).

$$TEv_{out} = TEv_{in} - \frac{\dot{Q}_{Ev}}{C_{Ev}} \tag{75}$$

After passing through the evaporator, the outlet air temperature is represented through Equation (75).

2.2. Condenser Section of the Heat Exchanger

The air conditioning is sucked through the exhaust pipes and passes through the heat pipe condenser region. The saturation temperature of the working fluid is higher than the temperature of the air conditioning, which varies between 0˚C and 15˚C. The inlet volume flow rate of the air conditioning in the condenser region varies between 0.1028 m^3/s and 0.1472 m^3/s.

The formulation used to simulate the heat exchange process in the condenser is established through Equations (76)-(92).

$$TCd_{in} = 0.0^{\circ}\mathrm{C};\ 0.0^{\circ}\mathrm{C} \le TCd_{in} \le 15.0^{\circ}\mathrm{C} \tag{76}$$

The air temperature at the condenser inlet, TCd_{in}, is represented by Equation (76).

$$\Delta T_{Cdsat} = T_{sat} - TCd_{in} \tag{77}$$

Equation (77) represents the temperature difference between the air and the working fluid in the Condenser.

$$LCd = LEv \tag{78}$$

The length of the condenser section, LCd, is represented through Equation (78).

$$LCd_{effec} = LCd - NFin\left(t_{Fin} + Sp_{Fin}\right) \tag{79}$$

Equation (79) represents the effective length of the condenser for heat exchange.

$$Dh_{Cd} = \frac{4WHE \times LCd_{effec}}{2\left(WHE + LCd_{effec}\right)} \tag{80}$$

The hydraulic diameter in the region of the capacitor, Dh_{Cd}, is represented

by Equation (80).

$$Re_{air} = \frac{4\dot{m}_{air}}{\pi Dh_{Cd}\mu_{air}} \tag{81}$$

The Reynolds number of air in the condenser region, Re_{air}, is represented through Equation (81).

$$Asec_{air} = \frac{\dot{m}_{air} Dh_{Cd}}{Re_{air}\mu_{air}} \tag{82}$$

The airflow area in the Condenser, $Asec_{air}$, is given by Equation (82).

$$h_{Cond} = 0.943\left[\frac{\rho_l\left(\rho_l - \rho_v\right)h_{lv}gk_W^3}{\mu_W LCd\Delta T_{sat}}\right]^{1/4} \tag{83}$$

The condensation transfer coefficient in the heat pipe, h_{Cond}, is given by Equation (83), as reported in [5].

$$Uo_{Cd} = \frac{1}{\frac{1}{h_{Cond}} + \frac{D_{ext} - D_{int}}{kW} + \frac{1}{\eta'_{Fin}h_{air}}} \tag{84}$$

Equation (84) represents the global heat transfer coefficient.

$$C_{Air} = \dot{m}_{air}Cp_{air} \tag{85}$$

$$C_{Cd} = C_{air} \tag{86}$$

The heat capacity of the air in the region of the condenser, C_{Cd}, is represented by Equation (86).

$$NTU_{Cd} = \frac{Uo_{Cd}A_{Total}}{C_{Cd}} \tag{87}$$

Equation (87) represents the number of thermal units associated with the heat pipes in the condenser region.

$$Fa_{Cd} = \frac{NTU_{Cd}}{2} \tag{88}$$

The dimensionless parameter called "fin analogy" in the condenser region, Fa_{Cd}, is represented through Equation (88).

$$\eta_{TCd} = \frac{\tanh\left(Fa_{Cd}\right)}{Fa_{Cd}} \tag{89}$$

Equation (89) represents the thermal efficiency associated with the condenser.

$$\varepsilon_{TCd} = \frac{1}{\frac{1}{\eta_{TCd}NTU_{Cd}} + \frac{1}{2}} \tag{90}$$

Equation (90) represents the thermal effectiveness related to the condenser.

$$\dot{Q}_{Cd} = \frac{C_{Cd}\Delta T_{Cdsat}}{\frac{1}{\eta_{TCd}NTU_{Cd}} + \frac{1}{2}} \tag{91}$$

The heat transfer rate between the air and the heat pipe in the Condenser re-

gion is represented by Equation (91).

$$TCd_{out} = \frac{\dot{Q}_{Cd}}{C_{Cd}} + TCd_{in} \tag{92}$$

The air outlet temperature in the Condenser, TCd_{out}, is represented through Equation (92).

2.3. Individually Finned Heat Pipe Crow-Flow Heat Exchanger—IFHPHE

The cooling and energy recovery set to form a heat exchanger, with a fresh air inlet with a temperature above 17˚C and a cooled air outlet below 17˚C. The total heat transfer rate in the air conditioning process is equal to the sum of the heat transfer rates in the evaporator and the condenser $\dot{Q}_{Cd}$, according to Equation (93). Equation (94) represents the maximum transfer rate, $\dot{Q}_{Max}$, in the heat exchanger, which $C_{\min}$ is the smallest of the thermal capacities of the air involved in the process. Equation (95) represents the heat exchanger's effectiveness in the air conditioning process.

$$\dot{Q}_{FHPHE} = \dot{Q}_{Ev} + \dot{Q}_{Cd} \tag{93}$$

$$\dot{Q}_{Max} = C_{\min}\left(TEv_{in} - TCd_{out}\right) \tag{94}$$

$$\varepsilon_{FHPHE} = \frac{\dot{Q}_{FHPHE}}{\dot{Q}_{Max}} \tag{95}$$

3. Results and Discussions

3.1. Evaporator Section of the Heat Exchanger

The air velocity increases with the airflow, according to Equation (48), and with the number of fins, as a function of the smaller passage area, as shown in **Figure 2**. The most significant influence on the velocity is the number of fins. The speed tends to increase exponentially for a significantly large number of fins.

The Nusselt number, **Figure 3**, decreases with the air flow rate and is strongly influenced by the number of fins, with a similar growth trend as the velocity. The variation of the inlet temperature also has a significant effect on the growth of the Nusselt number.

The thermal effectiveness increases with the number of fins, **Figure 4**, and tends asymptotically towards a maximum value close to 70 fins. The effect of the number of heat pipes on thermal effectiveness is very significant, and **Figure 4** presents threshold values for the considered configuration, NPH = 7, and NPH = 49. The thermal effectiveness suffers slight variation with the variation of air flow rate. A thermally ideal design corresponds to a number of fins between 60 and 70 and a number of heat pipes equal to 49.

Figure 5 shows the heat transfer rate as a function of the number of fins and the number of heat pipes for an inlet temperature equal to 20˚C. Consistent with the thermal effectiveness already discussed, heat transfer rates reach threshold

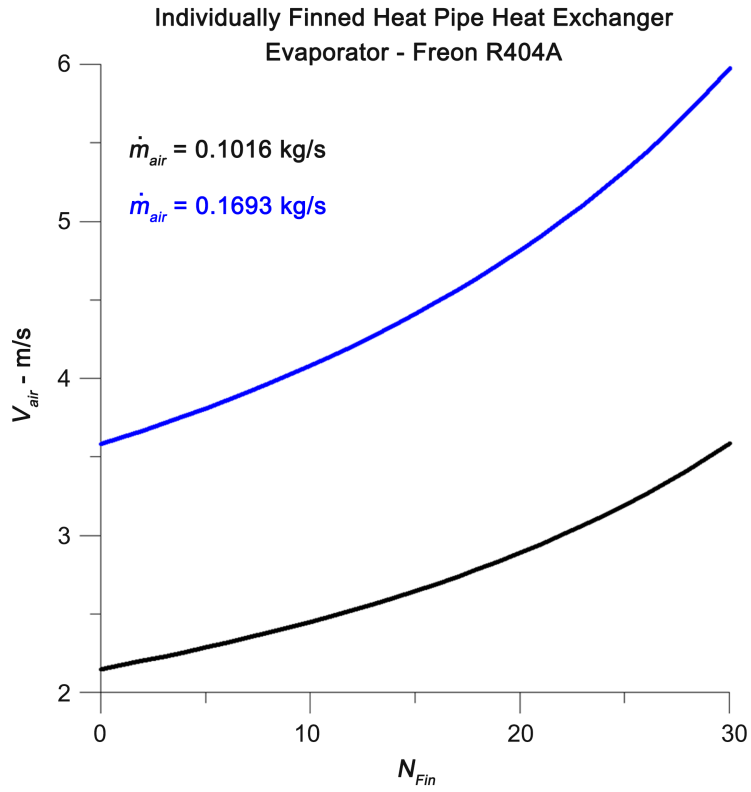

Figure 2. Air velocity at the evaporator section inlet versus the number of fins.

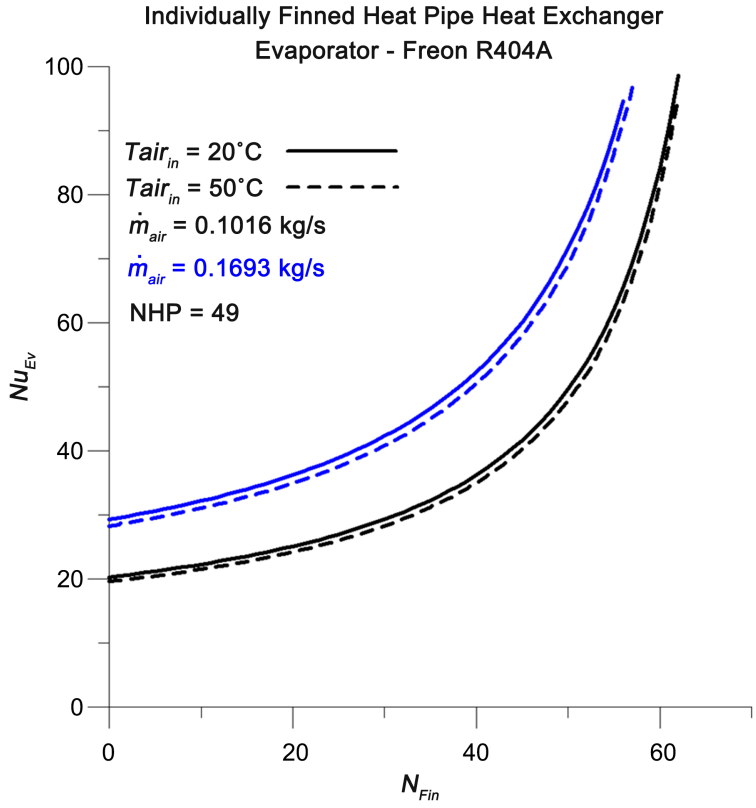

Figure 3. Nusselt number at the evaporator section versus the number of fins.

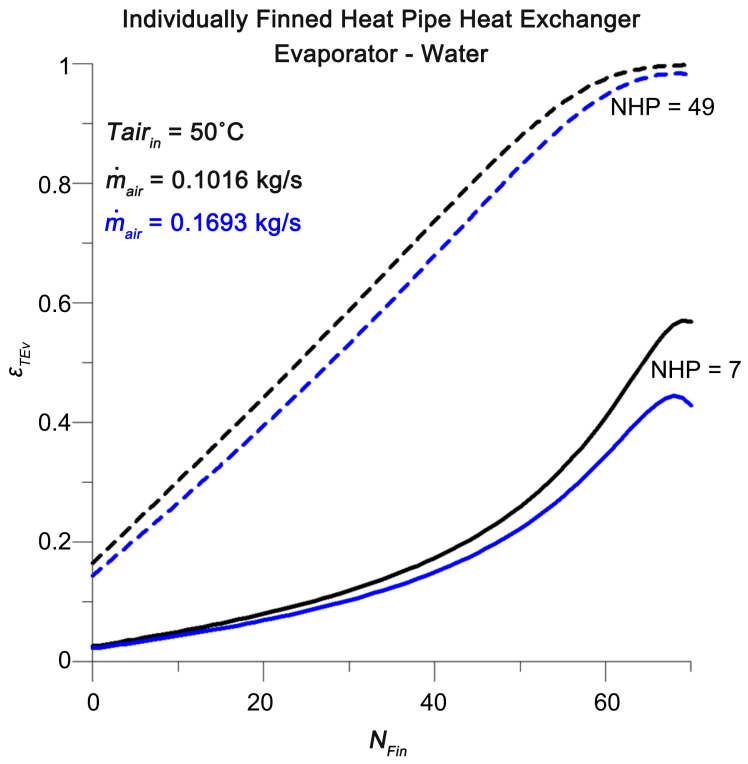

Figure 4. Thermal effectiveness at the evaporator section versus the number of fins and the number of heat pipes.

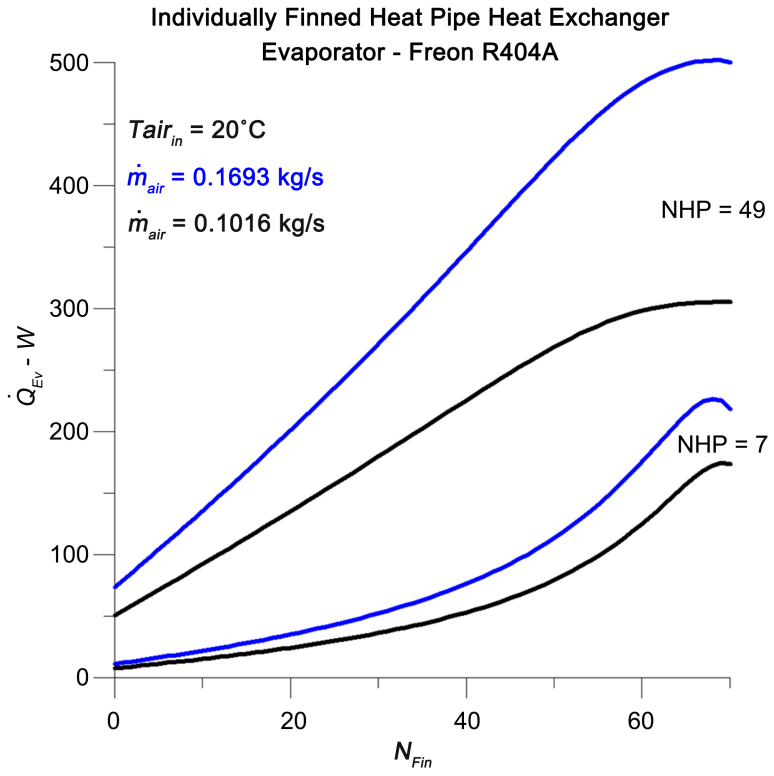

Figure 5. Heat transfer rate at the evaporator section versus the number of fins for $TEv_{in} = 20.0^{\circ}\mathrm{C}$.

values for numbers of fins between 60 and 70. The number of heat pipes dramatically influences the growth of the heat transfer rate, and the variation in the heat transfer rate with the mass flow rate of air is greater for a greater number of heat pipes. The fins and the number of heat pipes affect the heat exchange area, and the air flow rate affects the flow regime, which justifies the observed variations.

The results presented in Figure 6, when contrasted with Figure 5, demonstrate the effect of air inlet temperature variation on the heat transfer rate. For example, the heat transfer rate is more than ten times greater for an inlet temperature equal to 50˚C when compared with the heat transfer rate for an inlet temperature equal to 20˚C for the maximum number of heat pipes for the analyzed configuration, that is, 49 heat pipes.

The variation of the heat transfer rate as a function of the number of heat pipes is shown in Figure 7 for an inlet air temperature equal to 20˚C. It is observed that the heat transfer rate increases with the air flow rate, the number of fins, and the number of heat pipes. However, the number of fins per heat pipe is mainly responsible for the growth in heat transfer rate, followed by the number of heat pipes.

Results for air outlet temperatures as a function of inlet air temperature, number of fins, and heat pipes, can be observed in Figures 8-10. The outlet air temperature depends on the inlet air temperature, the number of fins, the number of heat pipes, and the airflow rate.

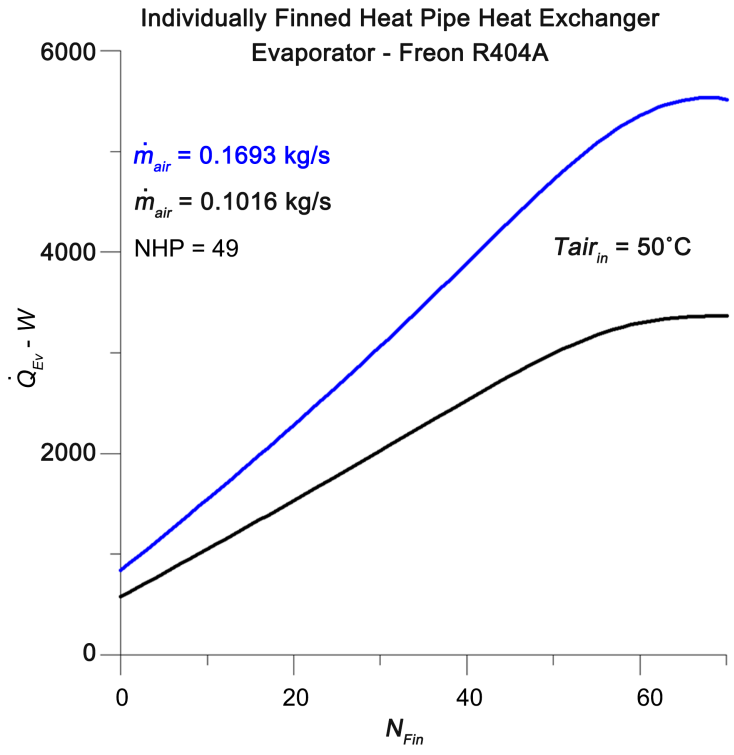

Figure 6. Heat transfer rate at the evaporator section versus the number of fins for $TEv_{in} = 50.0^{\circ}\mathrm{C}$.

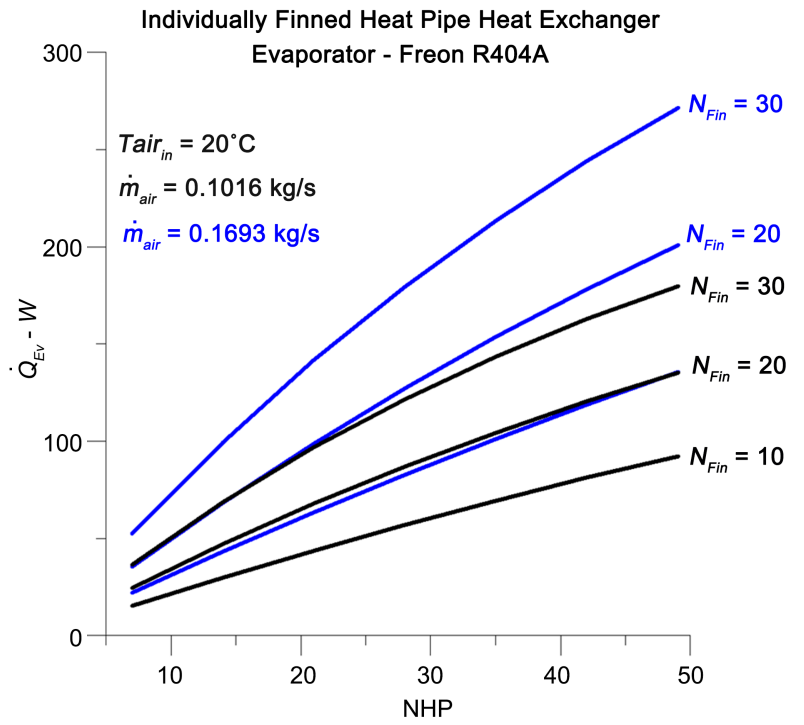

Figure 7. Heat transfer rate at the evaporator section versus the number of heat pipes for $TEv_{in} = 20.0^{\circ}\mathrm{C}$.

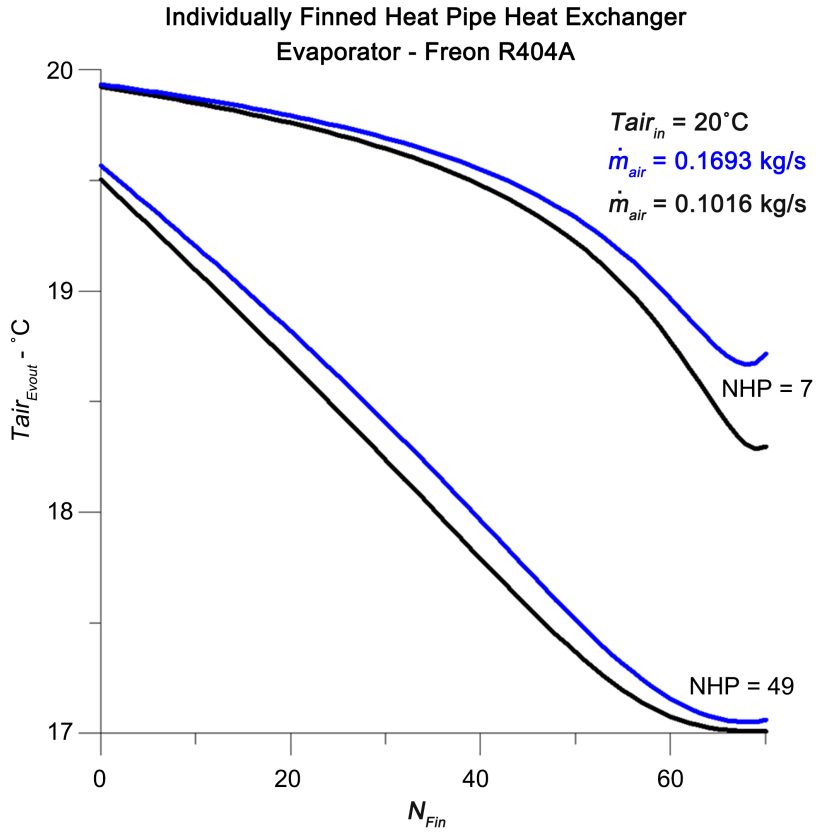

Figure 8. Air outlet temperature versus the number of fins for $TEv_{in} = 20.0^{\circ}\mathrm{C}$.

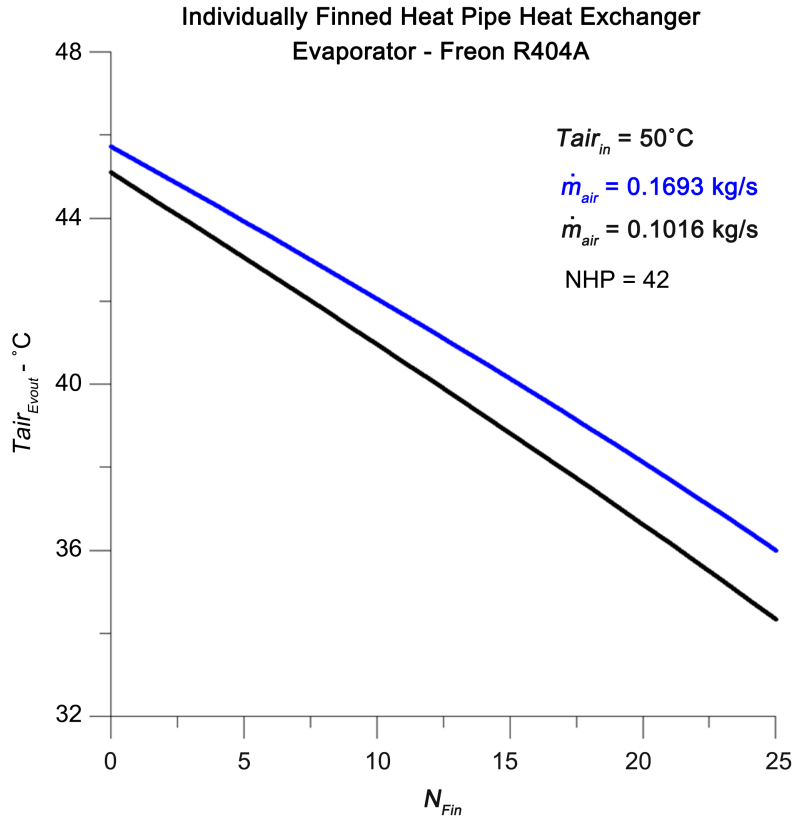

Figure 9. Air outlet temperature versus the number of fins for $TEv_{in} = 50.0^{\circ}\mathrm{C}$.

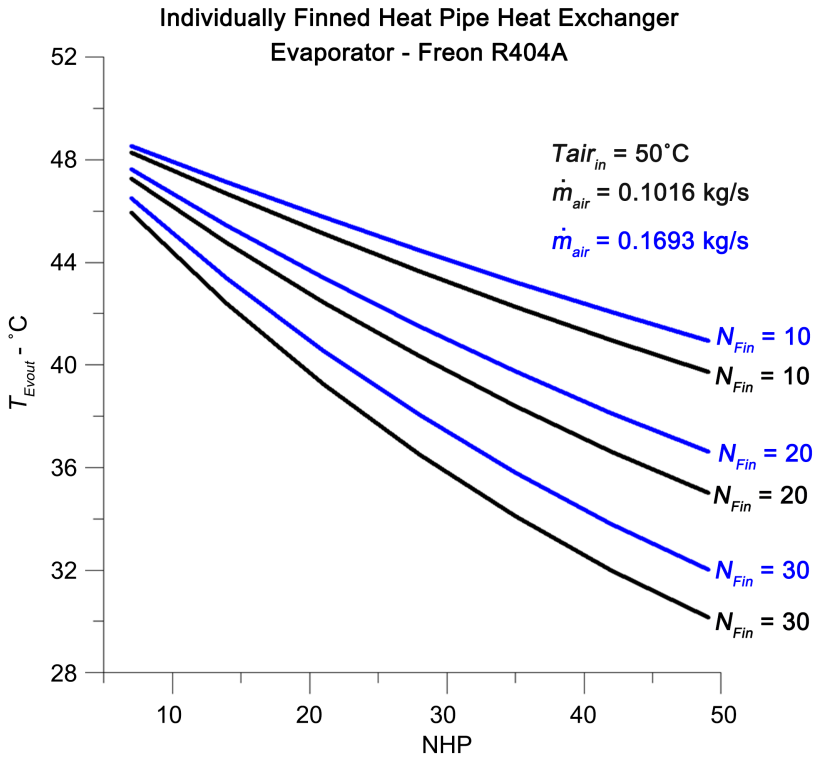

Figure 10. Air outlet temperature versus the number of heat pipes for $TEv_{in} = 50.0^{\circ}\mathrm{C}$.

Figure 8 demonstrates that, for air inlet temperature equal to 20˚C, the outlet temperature decreases with the number of fins and heat pipes, tending to the limit temperature when the number of fins is between 60 and 70. In this case, the outlet temperature of the air in the evaporator tends to the saturation temperature of the working fluid in the heat pipe.

Figure 10 presents results for air outlet temperature as a function of the number of heat pipes for an inlet temperature equal to 50˚C. When exploring the variation in the number of fins per heat pipe and the number of heat pipes, it becomes evident that the number of fins is a crucial parameter for improving thermal performance.

3.2. Condenser Section of the Heat Exchanger

The thermal effectiveness in the Condenser, analyzed through Figure 11, presents similar results to those obtained for the thermal effectiveness in the Evaporator, Figure 4, despite a slight variation in air flows. This similarity is justified by the fact that the heat exchanger geometry is the same in both regions, despite variations in inlet temperatures. Furthermore, when the number of fins per tube approaches 70, the number of limit heat tubes approaches 49. Therefore, in thermal terms, it can be said that these are the best heat exchanger performance numbers.

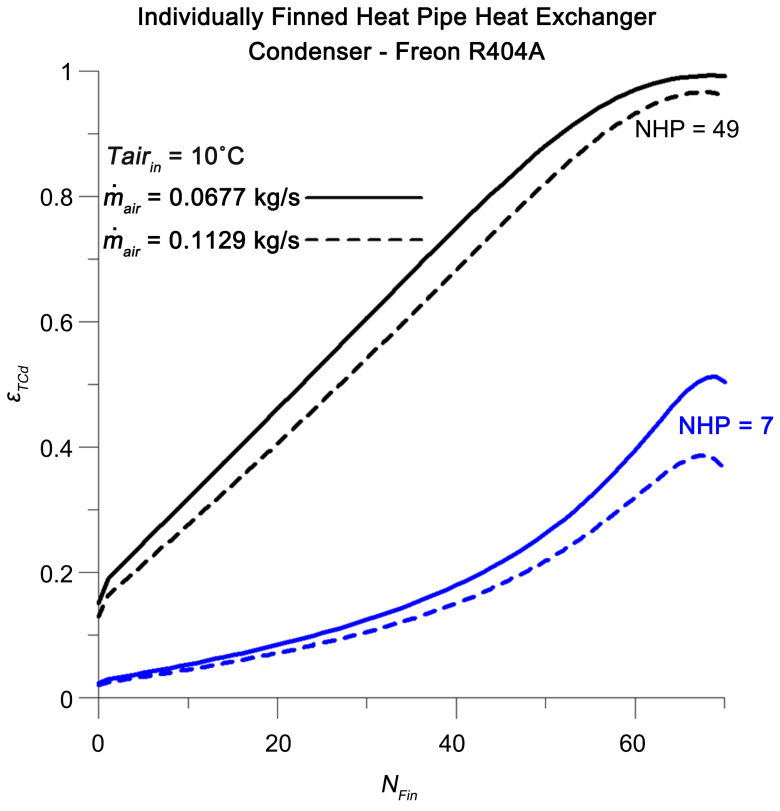

Figure 11. Thermal effectiveness at the condenser section versus the number of fins and the number of heat pipes for $TCd_{in} = 0.0^{\circ}\mathrm{C}$.

Figure 12 presents the evaporator air outlet temperature for two air inlet temperatures, 0˚C, and 10˚C. In this case, the number of fins per tube is equal to 30, and when the number of rows is equal to 21, the number of heat tubes corresponds to 49. As already observed, the air outlet temperature can be increased by placing greater fins per heat pipe.

3.3. Individually Finned Heat Pipe Crow-Flow Heat Exchanger—IFHPHE

The results obtained for the evaporator and condenser regions are physically and thermally consistent. It became evident that the number of fins per heat pipe is a crucial parameter to improve thermal performance, followed by the number of heat pipes. This last section compares the results obtained through the localized model with global experimental results for the heat exchanger obtained through reference [1]. To obtain the theoretical results, the number of 30 fins was imposed and the volumetric flows were removed from the reference ([1]; Table 3 pg. 19).

The effectiveness of the heat exchanger under analysis is represented in Figure 13, where the values obtained are reasonably close to the experimental values presented through reference [1], Figure 9, for the evaporator inlet temperature equal to 30˚C and inlet temperature of the condenser equal to 10˚C. The theoretical and experimental results are in better agreement with the high values of the number of heat pipes.

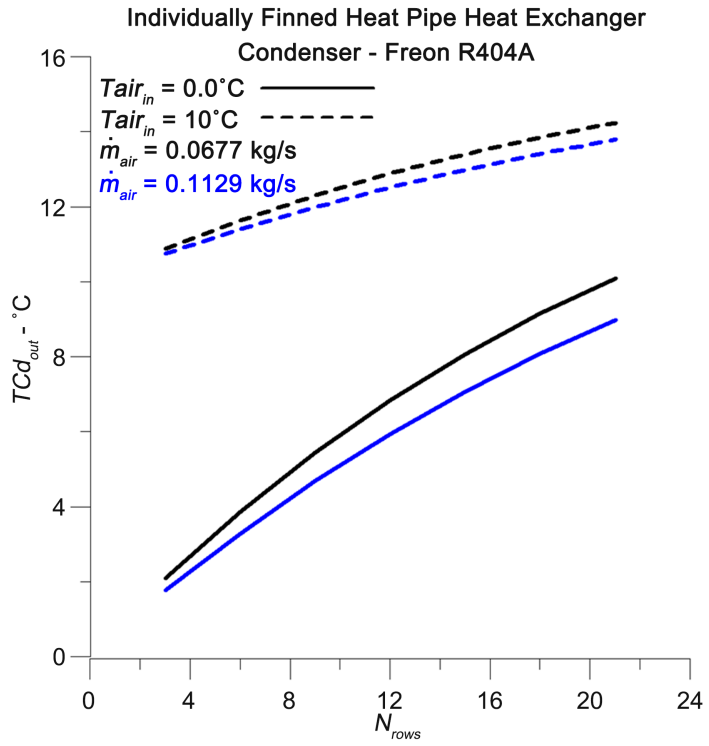

Figure 12. Condenser outlet temperature as a function of the number of rows of heat pipes for air inlet temperatures equal to 0˚C and 10˚C.

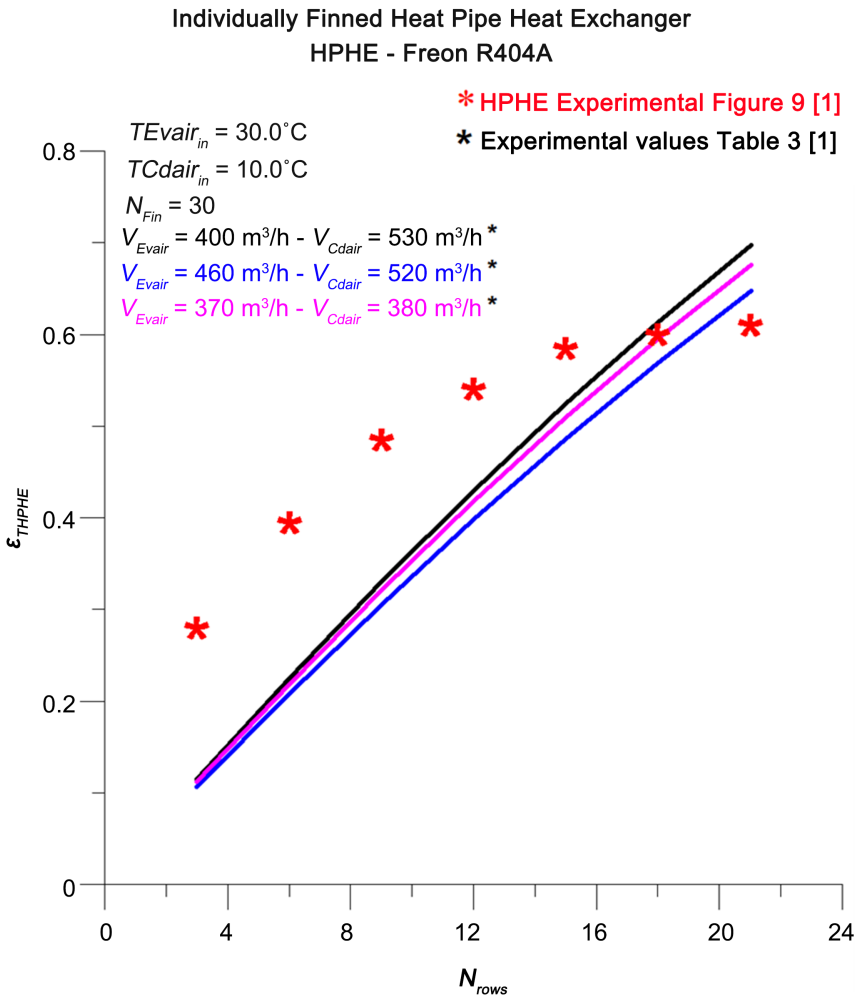

Figure 13. Thermal effectiveness for the IFHPHE versus the number of rows for $TEv_{in} = 30.0^{\circ}\mathrm{C}$ and $TCd_{in} = 10.0^{\circ}\mathrm{C}$.

The heat transfer rate to the heat exchanger as a function of the number of rows of heat pipes is shown in **Figure 14** for the conditions specified by the legends. The experimental values used for the theoretical versus experimental comparison were taken from **Figure 8** and reference ([1]; Table 3 pg. 19). In addition, the values obtained for the maximum heat transfer rate were also presented to evaluate the theoretical results better. Again, there is excellent agreement between theoretical and experimental results in a wide range of numbers of rows of heat pipes.

The heat transfer rate to the heat exchanger as a function of the air inlet temperature in the Condenser is shown in **Figure 15** for the conditions specified by the legends. The experimental values used for the theoretical versus experimental comparison were taken from ([1]; Figure 22 pg. 20) and ([1]; Table 3 pg. 19). Again, a good agreement between theoretical and experimental results is observed in the whole air inlet temperature range in the condenser analyzed in this work.

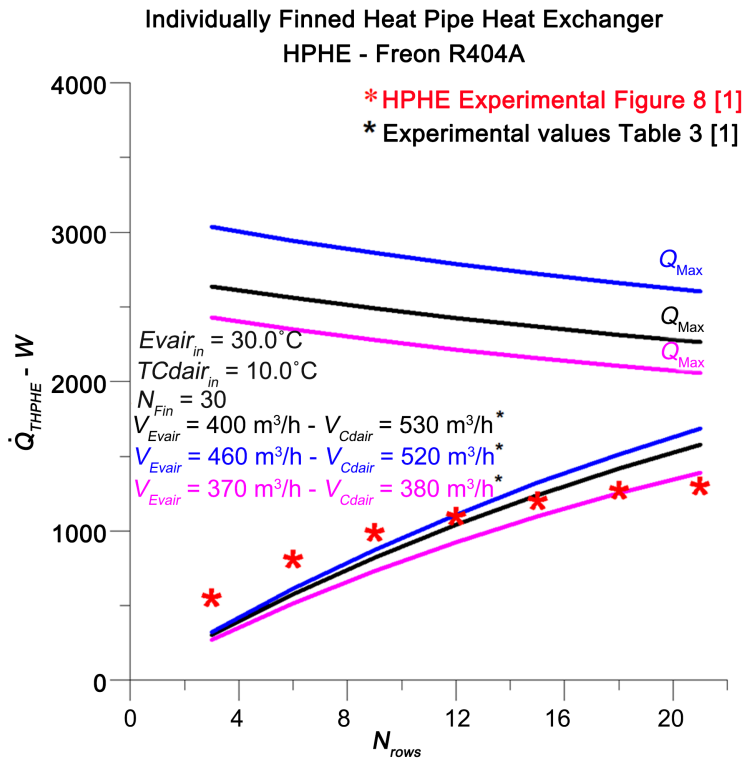

Figure 14. Heat transfer rate for the IFHPHE versus the number of rows for $TEv_{in} = 30.0^{\circ}\mathrm{C}$ and $TCd_{in} = 10.0^{\circ}\mathrm{C}$.

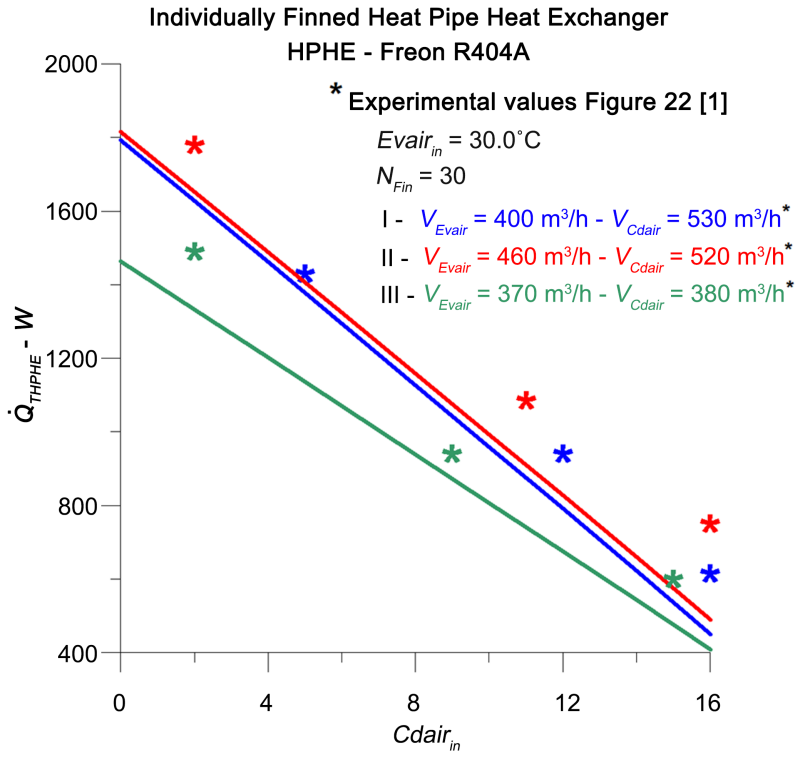

Figure 15. Heat transfer rate for the IFHPHE versus condenser inlet temperature for $TEv_{in} = 30.0^{\circ}\mathrm{C}$ and $TCd_{in} = 10.0^{\circ}\mathrm{C}$.

4. Conclusions

The results presented in this work when compared with experimental results, consolidate the theoretical localized approach for the heat exchanger and demonstrate that it can be an auxiliary tool for thermal performance analysis, including configurations and scope that, for an experimental procedure, can be expensive.

The main conclusions obtained through the work are:

- The results obtained for the evaporator and condenser regions are physically and thermally consistent. It became evident that the number of fins per heat pipe is a crucial parameter to improve thermal performance, followed by the number of heat pipes.
- There is excellent agreement between theoretical and experimental results in a wide range of numbers of rows of heat pipes.
- Good agreement between theoretical and experimental results is observed in the whole air inlet temperature range in the condenser analyzed in this work.

In this theoretical work, only the thermal performance of the heat exchanger was analyzed. A more comprehensive analysis, including aspects related to viscous dissipation, makes it possible to determine the cost-benefit ratio when analyzing the influence of the number of fins and the number of heat pipes. The thermodynamic Bejan number is the ideal parameter for this type of analysis.

Conflicts of Interest

The author declares no conflicts of interest regarding the publication of this paper.

References

[1] Górecki, G., Łęcki, M., Gutkowski, A.N., Andrzejewski, D., Warwas, B., Kowalczyk, M. and Romaniak, A. (2021) Experimental and Numerical Study of Heat Pipe Heat Exchanger with Individually Finned Heat Pipes. *Energies*, **14**, Article 5317. https://doi.org/10.3390/en14175317

[2] Putra, N.S.D., Anggoro, T. and Winarta, A. (2017) Experimental Study of Heat Pipe Heat Exchanger in Hospital HVAC System for Energy Conservation. *International Journal of Advance Science Engineering Information Technology*, **7**, 871-877. https://doi.org/10.18517/ijaseit.7.3.2135

[3] Jouhara, H., Almahmoud, S., Brough, D., Guichet, V., Delpech, B., Chauhan, A., Ahmad, L. and Serey, N. (2021) Experimental and Theoretical Investigation of the Performance of an Air to Water Multi-Pass Heat Pipe-Based Heat Exchanger. *Energy*, **219**, 119624. https://doi.org/10.1016/j.energy.2020.119624

[4] Hakim, I.I., Sukarno, R. and Putra, N. (2021) Utilization of U-Shaped Finned Heat Pipe Heat Exchanger in Energy-Efficient HVAC Systems. *Thermal Science and Engineering Progress*, **25**, 100984.https://doi.org/10.1016/j.tsep.2021.100984

[5] Sukarno, R., Putra, N., Hakim, I.I., Rachman, F.F. and Mahlia, T.Me.I. (2021) Multi-Stage Heat-Pipe Heat Exchanger for Improving Energy Efficiency of the HVAC System in a Hospital Operating Room. *International Journal of Low-Carbon Technologies*, **16**, 259-267. https://doi.org/10.1093/ijlct/ctaa048

[6] Jouhara, H., Chauhan, A., Nannou, T., Almahmoud, S., Delpech, B. and Wrobel, L.C. (2017) Heat Pipe Based Systems—Advances and Applications. *Energy*, **128**, 729-754. https://doi.org/10.1016/j.energy.2017.04.028

[7] Suleiman, A., Jamil, N. and Ameen, H.A. (2021) Thermal Performance of HAVC System Using Heat Pipe Heat Exchanger. *Journal of Mechanical Engineering Research and Developments*, **44**, 336-344. https://www.researchgate.net/publication/349350484

[8] Mostafa A. Abd El-Baky and Mousa M. Mohamed (2006) Heat Pipes Heat Exchanger for Heat Recovery in Air Conditioning. *Applied Thermal Engineering*, **27**, 795-801. https://www.researchgate.net/publication/260478732

[9] Barrak, A. (2021) Heat Pipes Heat Exchanger for HVAC Applications. In: Arais, M., Ed., *Heat Transfer—Design, Experimentation, and Applications*, IntechOpen, Baghdad, 1-14. https://doi.org/10.5772/intechopen.95530.

[10] Höhne, T. (2022) CFD Simulation of a Heat Pipe Using the Homogeneous Model. *International Journal of Thermofluids*, **15**, Article 100163. https://doi.org/10.1016/j.ijft.2022.100163

[11] Rohsenow, W.M. (1951) A Method of Correlating Heat Transfer Data for Surface Boiling of Liquids. M.I.T. Division of Industrial Cooporation, Cambridge. http://hdl.handle.net/1721.1/61431

[12] Fakheri, A. (2007) Heat Exchanger Efficiency. *Transactions of the ASME*, **129**, 1268-1276. https://doi.org/10.1115/1.2739620

[13] Nogueira, É. (2020) Thermal Performance in Heat Exchangers by the Irreversibility, Effectiveness, and Efficiency Concepts Using Nanofluids. *Journal of Engineering Sciences*, **7**, F1-F7. https://doi.org/10.21272/jes.2020.7(2).f1

[14] Nogueira, É. (2022) Thermo-Hydraulic Optimization of Shell and Externally Finned Tubes Heat Exchanger by the Thermal Efficiency Method and Second Law of Thermodynamics. *International Journal of Chemical and Process Engineering Research*, **9**, 21-41. https://doi.org/10.18488/65.v9i1.3130

Nomenclature

Asec—cross-section area
Atr—heat transfer area
Cp—specific heat
C—thermal capacity
$C_{\min}$ —minimum thermal capacity
D_h —hydraulic diameter
Fa—fin analogy
h—coefficient of heat convection
k—thermal conductivity
K—Kelvin
k_W —thermal conductivity of the tube
k_{Fin} —thermal conductivity of the fin,
L—vertical or horizontal length
$\dot{m}_{air}$ —mass flow rate of the air
N_{Fin} —number of fins
Nu—Nusselt number
Pr—Prandtl number
$\dot{Q}$ —actual heat transfer rate
$\dot{Q}_{\max}$ —maximum heat transfer rate
Re—Reynolds number
T—temperatures
Uo—global heat transfer coefficient

Subscripts

boil—ebulição
Cd—Condenser
Cond—Condenser
effect—effective
Ev—Evaporator
ext—external
HP—heat pipe
H—horizontal
in—inlet
int—internal
out—outlet
sat—saturation

Greek symbols

α—thermal diffusivity
β—the relationship between areas
ρ—density of the fluid
μ—dynamic viscosity of fluid
ν—kinematic viscosity of the cold fluid
ε_T—thermal effectiveness

η_T—thermal efficiency

ΔT—a difference of temperatures, [˚C]

Acronyms

FHPHE—Finned heat pipe heat exchanger

Ev—Evaporators

Cd—Condenser

NHP—Number of Heat Pipes

NFin—Number of Fins

Nrows—Number of rows

NTU—number of thermal units